

Supplementary information

Molecular insights into the *in situ* early-stage assembly of metal-organic frameworks on cellulose nanofibrils

Kailong Zhang,^a Micholas D. Smith^b and Mi Li^{*a}

^a Center for Renewable Carbon, School of Natural Resources, University of Tennessee, Knoxville, TN 37996, USA

^b Department of Biochemistry and Cellular and Molecular Biology, University of Tennessee, Knoxville, TN 37996, USA

* Corresponding author. Email: mli47@utk.edu

Table of Contents

Fig. S1 SEM images and model illustrations of TOCNF.

Fig. S2 FTIR and XRD of the synthesized TOCNF/MOF materials.

Fig. S3 Illustration of graph connected component used to identify MOF clusters.

Fig. S4 Representative clusters for each cluster size in $S_{\text{Hybrid-5}}$ system.

Fig. S5 Distribution of Zn ions in $S_{\text{MOF-small}}$ system showing convergence.

Fig. S6-S7 Frequency of identified cluster size in S_{MOF} and $S_{\text{Hybrid-5}}$ systems.

Fig. S8 Coordination analysis between Zn ions and TOCNF.

Fig. S9-S10 Frequency of clusters attached to TOCNF via coordination and hydrogen bonds.

Fig. S11 Effect of different precursor concentrations on the formation of MOF clusters.

Table S1 Force field parameters for the dummy model of zinc ions.

Table S2 Summary of simulation systems.

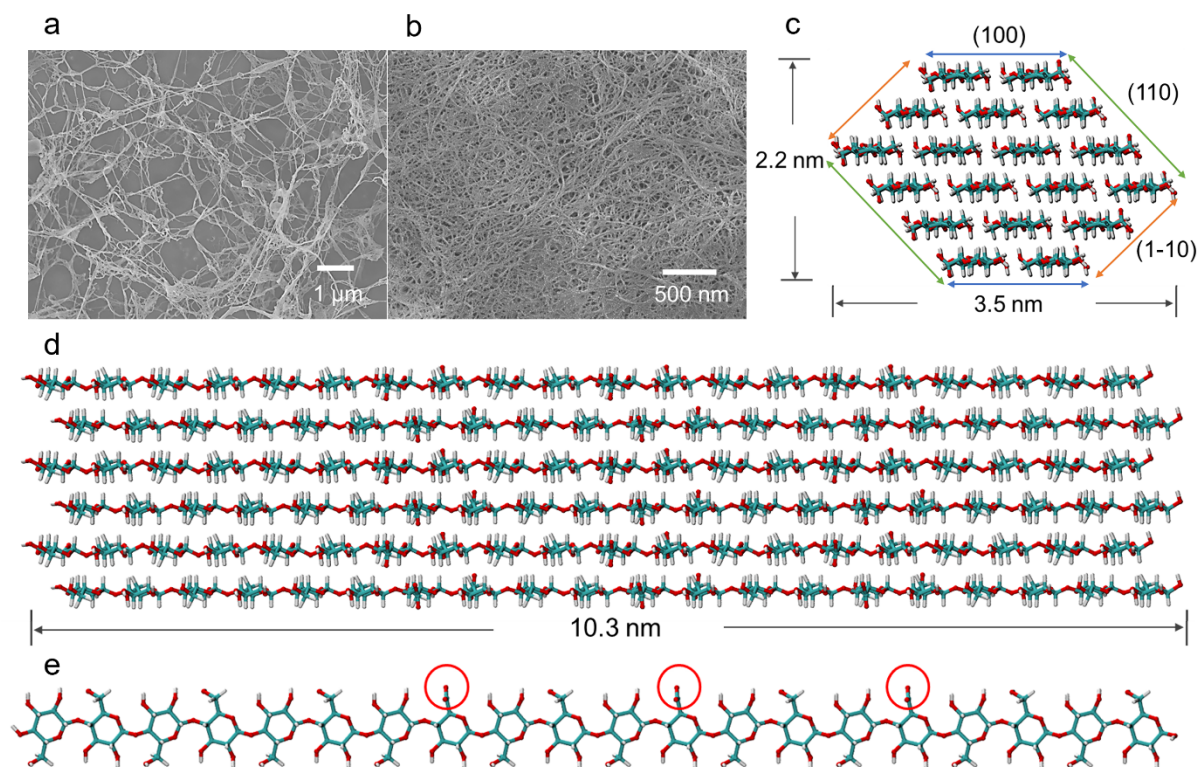


Fig. S1 SEM images of pristine TOCNF (a) and crosslinked TOCNF (b). Illustration of the 18-chain TOCNF model: Cross-section depicting the crystalline I β structure with the (100), (110), and (1-10) planes (c); Longitudinal view of the (100) plane showing the fibril composed of 20 D-glucose monomers (d); A single outer layer chain with three C6 hydroxyl groups modified into carboxylate groups (e).

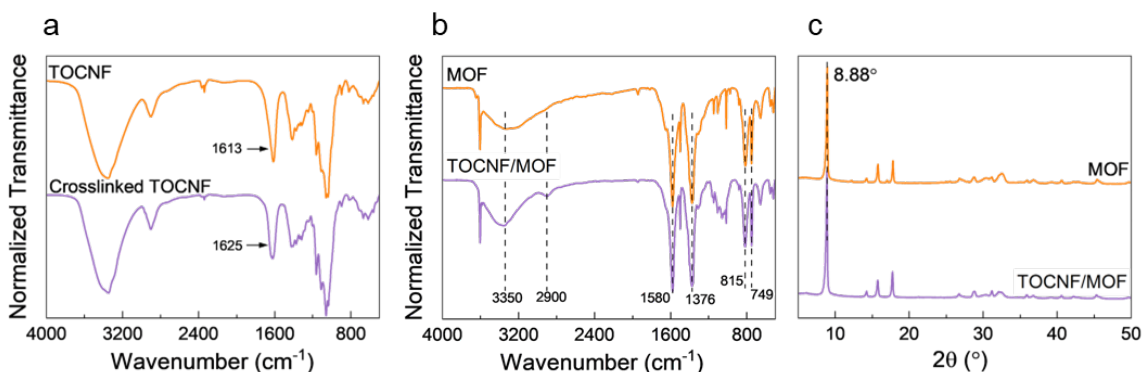


Fig. S2 FTIR spectra of TOCNF and crosslinked TOCNF (a) and MOF and TOCNF/MOF hybrid (b). XRD patterns of MOF and TOCNF/MOF hybrid (c).

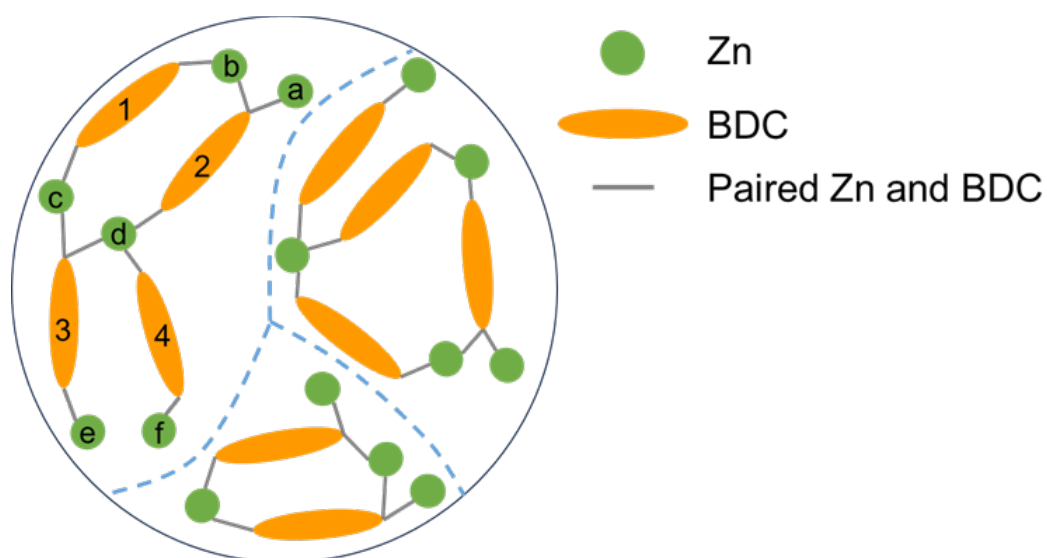


Fig. S3 Illustration of Zn-BDC cluster identification using graph-connected component theory.¹ The connected graph is searched and identified using in-house Python code. In this graph-based representation, each cluster is depicted as a connected component, where any node within the component can reach any other node via a connecting path. A Zn-BDC pair is considered to form a bridge when the distance between BDC and Zn nodes is less than 2.5 Å, according to RDF analysis. For example, node a and node c belong to the same cluster component, as there is a path a-2-b-1-c connecting them. The illustration demonstrates three separate cluster components.

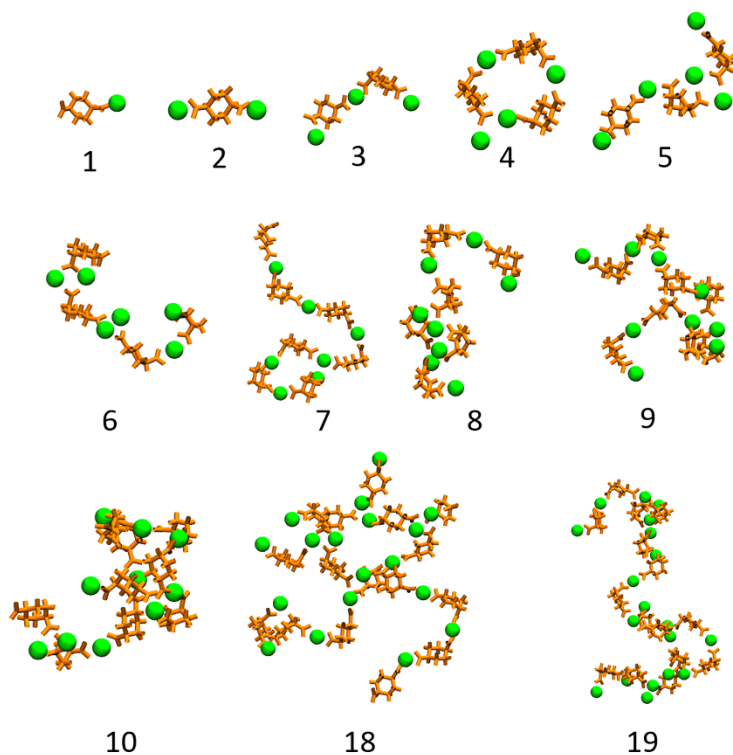


Fig. S4 Snapshots showing representative clusters for each cluster size at 150 ns in $S_{\text{Hybrid-5}}$ system.

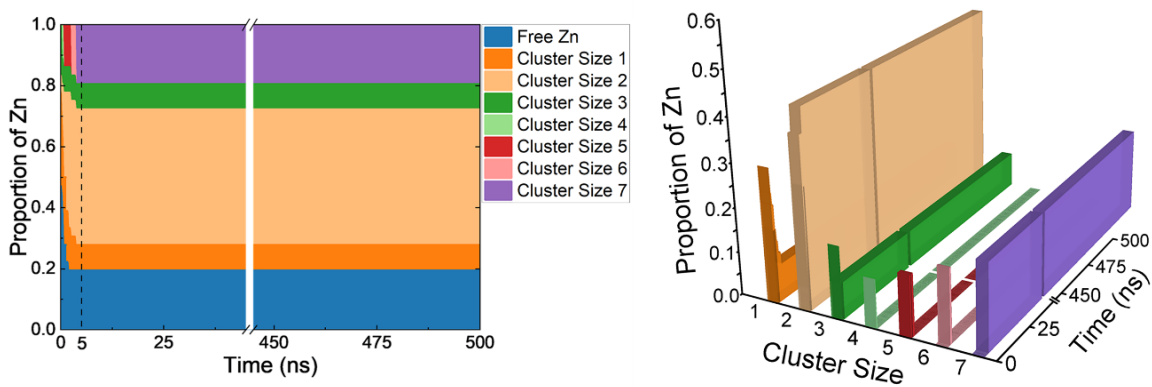


Fig. S5 The distribution of Zn ions in different cluster fractions over time in $S_{\text{MOF-small}}$. The system converged within 5 ns.

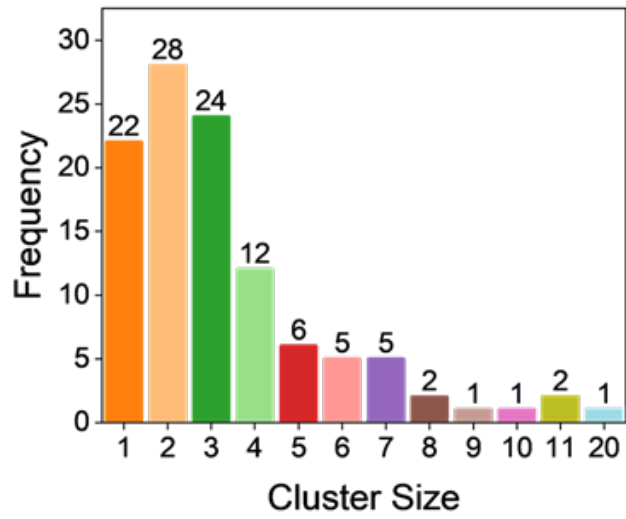


Fig. S6 Frequency of identified cluster size at 150 ns in S_{MOF} system.

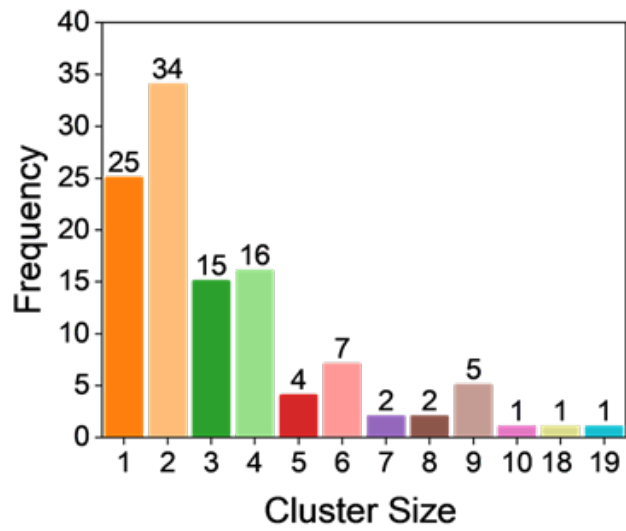


Fig. S7 Frequency of identified cluster size at 150 ns in S_{Hybrid-5} system.

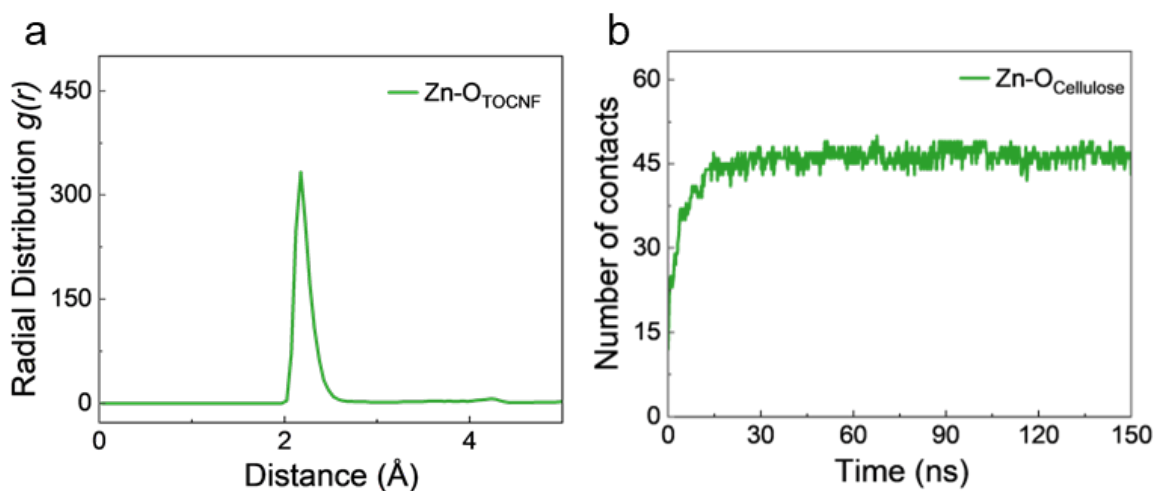


Fig. S8 Radial distribution function (a) and number of contacts between Zn ions and oxygen atoms in the carboxylate groups of TOCNF (b). Radial distribution function is calculated from 140 ns to 150 ns. Analysis is derived from the S_{Hybrid-5} system.

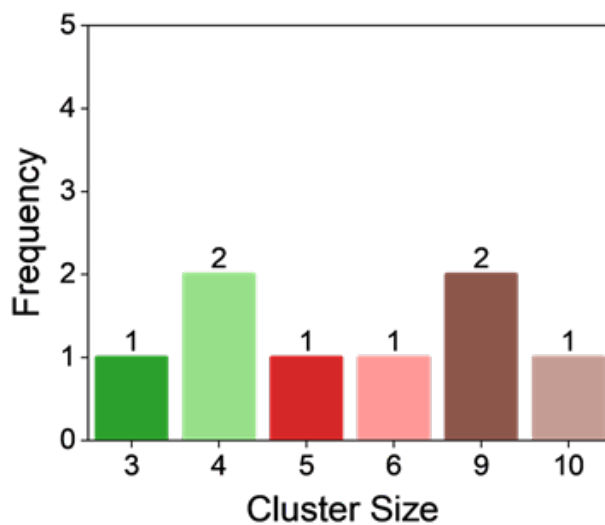


Fig. S9 Frequency of identified cluster size attached to TOCNF via coordination bond at 150 ns in S_{Hybrid-5} system.

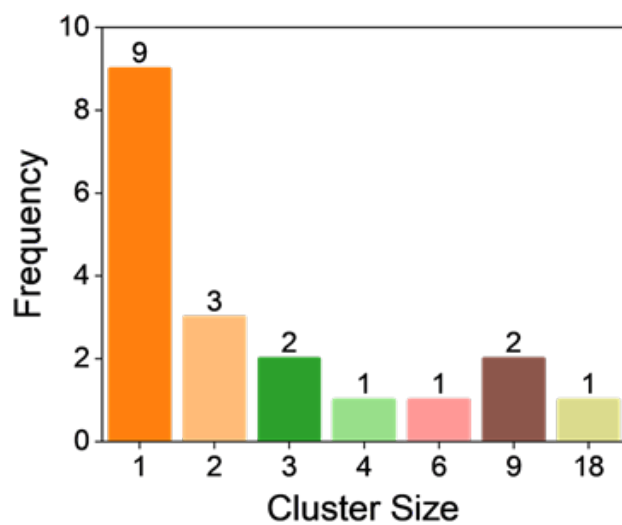


Fig. S10 Frequency of identified cluster size attached to TOCNF via hydrogen bond at 150 ns in $S_{\text{Hybrid-5}}$ system.

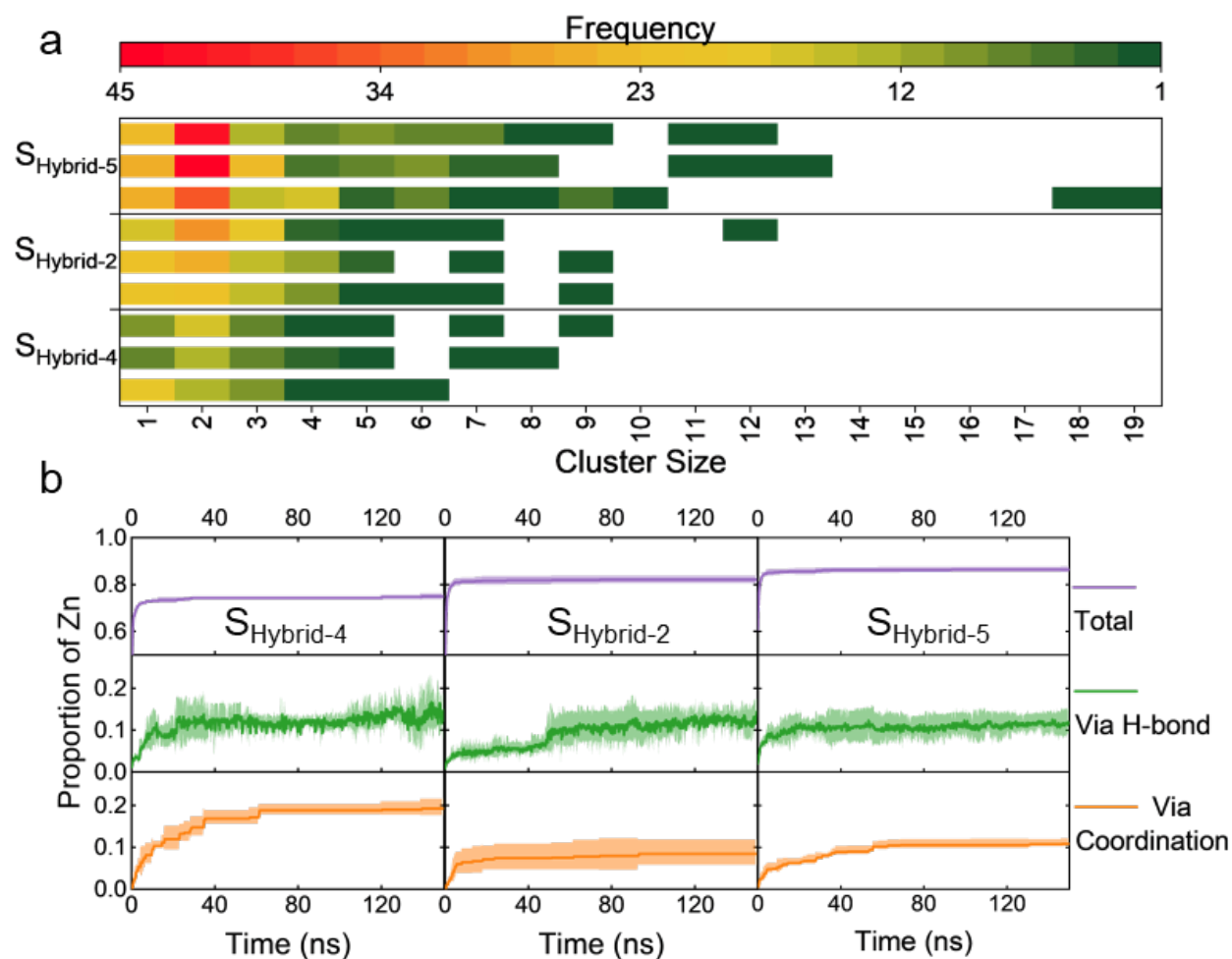


Fig. S11 Effect of different precursor concentrations on the formation of cluster sizes at 150 ns. Data are presented as three individual replicates for each system (a). Effect of the precursor concentration on the distribution of Zn ions in various cluster fractions. The yellow line represents clusters attached to TOCNF via coordination bond, the green line represents clusters attached to TOCNF via hydrogen bond, and the purple line represents the total clusters formed in the system. Data are presented as mean \pm standard deviation from three replicates (b). The analysis is based on the $S_{\text{Hybrid-4}}$, $S_{\text{Hybrid-2}}$, and $S_{\text{Hybrid-5}}$ systems, with concentrations increasing in a ratio of 1:2:4 based on the number of BDC ligands.

Table S1 Force field parameters for the dummy model of zinc ions. The parameters are derived from previously published work.²

Bond type	b_0 (Å)	K_b (kcal/mol Å ²)		
Zn-D	0.900	800.0		
Angle type	θ_0 (degree)	K_θ (kcal/mol rad ²)		
Di—Zn—Di	180.0	250.0		
Di—Zn—Dj	90.0	250.0		
Atom type	Mass	Charge (e)	σ_{ZnO} (Å)	ϵ_{ZnO} (kcal/mol)
Zn	47.370	-1.00	2.088	4.2386
D	3.000	0.50	$\sigma_D = 0$	$\epsilon_D = 0$

Table S2 Summary of simulation systems with various combinations of TOCNF, Zn ion, BDC, and acetate. The simulations for $S_{Hybrid-1}$ through $S_{Hybrid-5}$ were conducted in triplicate.

System	Number of TOCNF	Number of Zn ions	Number of BDC ligands	Number of acetates	Solvent	Box dimension (nm ³)	Trajectory length (ns)
S _{MOF-small}	0	36	24	24		6	500
S _{MOF}	0	432	288	288			
S _{Hybrid-1}		198	144	72			
S _{Hybrid-2}	1 (with 36 carboxylates)	234	144	144	DMF	14	150
S _{Hybrid-3}		270	144	216			
S _{Hybrid-4}		126	72	72			
S _{Hybrid-5}		450	288	288			

References

1. K. Gura, J. L. Hirst and C. Mummert, *Computability*, 2015, **4**, 103-117.
2. Q. Liao, S. C. L. Kamerlin and B. Strodel, *J. Phys. Chem. Lett.*, 2015, **6**, 2657-2662.